

Oscillatory Instabilities in the Electrooxidation of Borohydride on Platinum

Eduardo G. Machado and Hamilton Varela*[‡]

Institute of Chemistry of São Carlos, University of São Paulo,
CP 780, 13560-970 São Carlos-SP, Brazil

O íon boroidreto tem se mostrado um promissor combustível alternativo. Grande parte das pesquisas aborda o aspecto electrocatalítico da electrooxidação deste combustível sobre platina e ouro. Apesar das conhecidas limitações cinéticas e do intrincado mecanismo, nosso Grupo relatou recentemente a ocorrência de duas regiões de biestabilidade e autocatálise no potencial do eletrodo durante a interação em potencial de circuito aberto entre este íon e a superfície de platina oxidada. Seguindo esta contribuição, neste trabalho fenômenos ainda mais complicados são apresentados: a presença de oscilações electroquímicas durante a electrooxidação do íon boroidreto em platina em meio alcalino. Oscilações de corrente foram associadas a duas janelas distintas de instabilidades e caracterizadas no plano de potencial-resistência. As características dinâmicas de tais oscilações sugerem a existência de mecanismos distintos de acordo com a região de potencial. Resultados publicados anteriormente obtidos sob regime não-oscilatório foram usados para fornecer algumas dicas sobre as reações superficiais por trás da dinâmica observada.

The borohydride ion has been pointed as a promising alternative fuel. Most of the investigation on its electrochemistry is devoted to the electrocatalytic aspects of its electrooxidation on platinum and gold surfaces. Besides the known kinetic limitations and intricate mechanism, our Group has recently found the occurrence of two regions of bi-stability and autocatalysis in the electrode potential during the open circuit interaction of borohydride and oxidized platinum surfaces. Following this previous contribution, the occurrence of more complicated phenomena is here presented: namely the presence of electrochemical oscillations during the electrooxidation of borohydride on platinum in alkaline media. Current oscillations were found to be associated to two distinct instability windows and characterized in the resistance-potential parameter plane. The dynamic features of such oscillations suggest the existence of distinct mechanisms according to the potential region. Previously published results obtained under non-oscillatory regime were used to give some hints on the surface chemistry behind the observed dynamics.

Keywords: borohydride electrooxidation, current oscillations, N-NDR oscillators

Introduction

Borohydride has been pointed as a promising molecule due to its potential use as alternative energy source. During its electrooxidation, 8 electrons are released and the reversible thermodynamic potential of the reaction is -1.24 V vs. NHE. Additionally, sodium borohydride is solid at room temperature and can be used in direct fuel cells or in fuel cells as hydrogen source. It is easy to store, has high power density and its final oxidation product, BO_2^- can be converted again to BH_4^- .¹⁻³ Despite all advantages, the usage of this fuel presents some drawbacks, posed mainly

by its homogeneous and heterogeneous hydrolysis, which considerably lowers the number of electrons released in the direct oxidation path.

Important mechanistic aspects on the processes involved in the electrooxidation of borohydride have been recently surfaced.⁴⁻⁷ Nevertheless, the picture is still incomplete and it seems there are still some unknown intermediates, which are not identifiable by spectroscopy.⁸ Finkelstein *et al.*⁹ argue that there are two forms of direct BH_4^- oxidation, one at low potentials yielding $7e^-$ and other at high potentials yielding $5-6e^-$. Gyenge⁶ proposed that the oxidation occurs depending on the adsorption of BH_4^- and intermediates and the interaction among them. Liu *et al.*¹⁰ have reviewed alternate pathways for this reaction and argue that the anodic reaction of borohydride may be different

*e-mail: varela@iqsc.usp.br

[‡]Present address: Fritz Haber Institute of the Max Planck Society, Department of Physical Chemistry, Faradayweg 4-6, D-14195 Berlin, Germany

according to the conditions of the reaction and the type of electrocatalyst. Despite the efforts of many scientists, the mechanism of BH_4^- oxidation remains incomplete to date and it is clear that the efficient use of BH_4^- as a fuel is not yet possible.

We have recently tackled the problem of the open circuit interaction between borohydride and oxidized platinum surface.¹¹ From the applied side, this experimental approach is important because it mimics the fuel crossover from the anode to the cathode that severely decreases the fuel cell performance.¹²⁻¹⁵ From the fundamental point of view, this study allowed us to describe two processes of autocatalytic production of free platinum sites and to correlate these regions with those found in the cyclic voltammogram. In the present contribution, we deepened our investigation on the nonlinear aspects of the electrooxidation of borohydride on platinum and describe, for the first time, the occurrence of self-organized current oscillations in two specific potential regions.

Experimental

As working electrode, a spherical shaped platinum electrode with an active area of 0.21 cm^2 , as measured by the hydrogen oxidation region, was used. The supporting electrolyte was a 1.0 mol L^{-1} NaOH (Sigma-Aldrich, 99.99%) solution, as to minimize the homogeneous hydrolysis of the borohydride ion.⁶ A high area golden sheet was used as a counter electrode, aiming at minimizing the heterogeneous hydrolysis of the ion in comparison to a platinum sheet.¹⁶ All potentials were quoted vs. the reversible hydrogen electrode (RHE) prepared with the electrolyte solution. Before and during all experiments, argon (99.996%, White Martins®) was purged into the system to avoid any interference from dissolved oxygen. All solutions were prepared using ultra-pure Millipore® water ($18.2 \text{ M}\Omega \text{ cm}$). For all the experiments, the concentration of the borohydride (NaBH_4 , Sigma-Aldrich, 95%) solution was 5 mmol L^{-1} . It was used a one-chambered cell.

Before each experiment, the working electrode was annealed with a butane flame for about 1 min. After cooling in argon atmosphere, the electrode was inserted into the solution and the potential was cycled between 0.05 and 1.5 V for 100 times at 1.0 V s^{-1} for an electrochemical cleaning. The potential was then cycled at the same window, but at 100 mV s^{-1} to check the cleanness of the system. Only then the borohydride solution was added into the system.

The electrochemical experiments were accomplished using an Autolab® potentiostat (model PGSTAT302N) equipped with a Scan-Gen module (analog scan generator). Data acquisition was $0.0028 \text{ s per point}$. Experiments

were performed with stagnant solution, and at $25 \pm 1 \text{ }^\circ\text{C}$, controlled by a thermostat.

Results and Discussion

Figure 1 shows a typical cyclic voltammogram for the electrooxidation of borohydride on platinum in alkaline medium. The main features of the voltammetric profile have been discussed elsewhere,^{7,9,17,18} herein the focus is on the electrochemical instabilities. The most common signature of instabilities in electrochemical systems is the occurrence of a negative differential resistance (NDR)¹⁹⁻²² in the current-potential curve. Two particular NDR are discernible in Figure 1: the first one around 0.6-0.8 V and the second one above 1.2 V. We have correlated the occurrence of a two-step transition observed during the open circuit interaction between borohydride and an oxidized platinum surface with these two NDR.¹¹ The autocatalytic production of free platinum sites described for each step was tentatively associated to the specific surface chemistry of adsorbates in that potential window. At each potential region, the system presents bi-stability, which in its turn reflects the co-existence of two stable states for a given parameter interval. Both NDR regions depicted in Figure 1 are connected to N-shaped current-potential feature (although only part of the 'N' is shown for the second, more positive potential region). In such systems, the electrode potential (ϕ) plays the role of an autocatalytic variable in the positive feedback loop.

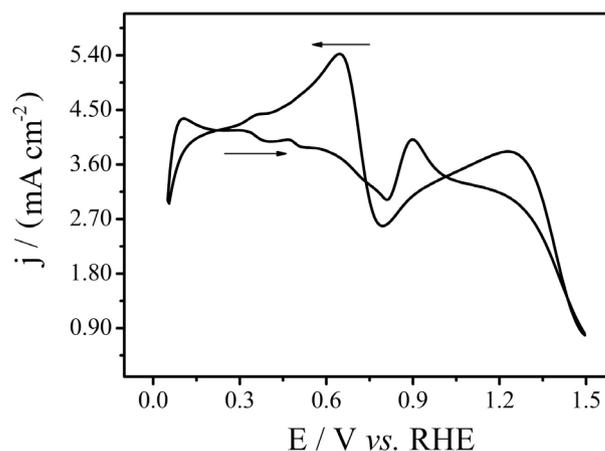


Figure 1. Cyclic voltammogram (at 100 mV s^{-1}) of the electrooxidation of borohydride on platinum. Electrolyte: aqueous 1 mol L^{-1} NaOH solution containing 5 mmol L^{-1} BH_4^- .

Bi-stability in N-NDR systems becomes more evident when the N-shaped curve is folded in such a way that the two stable states overlap in a certain potential window. This occurs when the total resistance of the system reaches a

certain critical value. Figure 2 illustrates a quasi-stationary potentiodynamic sweep in the presence of an external resistance (R_{ext}) of 1 k Ω connected between the working electrode and the potentiostat. The whole (continuous line) curve is shifted to more positive potentials as a consequence of the insertion of the external resistance, or of the ohmic drop. Under these experimental conditions, the two NDR appear now at about 1.25 and 1.5 V and are clearly folded. The main characteristics to be stressed here are the current spikes observed in each region. Presenting now the data in terms of the actual ϕ , *cf.* the dotted line in Figure 2, the NDR regions occur at about the same potential region. In this plot, ϕ was obtained by subtracting the ohmic drop term, IR (where I stands for the current), from the applied potential E , i.e., $\phi = E - IR$, where R is the total resistance, which subsumes the external (R_{ext}) and the solution (R_s) resistances. In our experiments, R_s was typically about 5 Ω , so that R_{ext} presents the main contribution to R in all cases studied here.

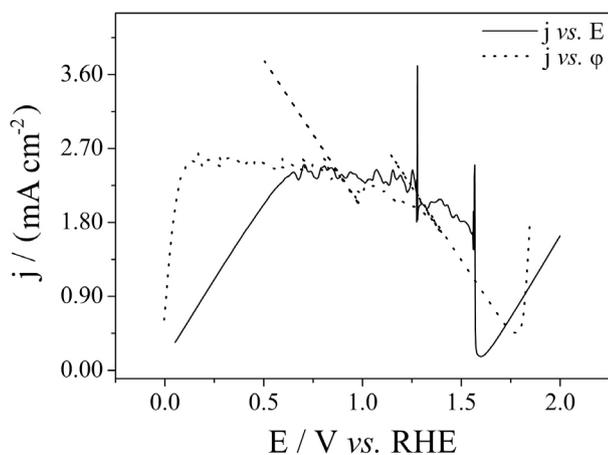


Figure 2. Slow potentiodynamic sweep (at 1 mV s⁻¹) of the electrooxidation of borohydride on platinum in the presence of an external resistance (R_{ext}) of 1 k Ω connected between the working electrode and the potentiostat. Full line represents the as-obtained results, whereas the data with the current given as a function of the working electrode potential ($\phi = E - IR$, or $\phi = E - jAR$) are given in the dotted line. See text for details. Remaining experimental conditions as in Figure 1.

In order to explore the nature of the current spikes present in Figure 2, the current evolution in potentiostatic experiments at E fixed around the two NDR regions was studied. Figure 3 shows typical results for (a) the first and (b) the second NDR region. In these experiments, the electrode potential was stepped from the open circuit potential to the one of interest. For the first NDR region, oscillations are exemplified for (a1) $E = 1.30$ V and (a2) $E = 1.33$ V. These relation-like oscillations have frequencies in the range between 0.1-0.5 Hz and were found to start abruptly.

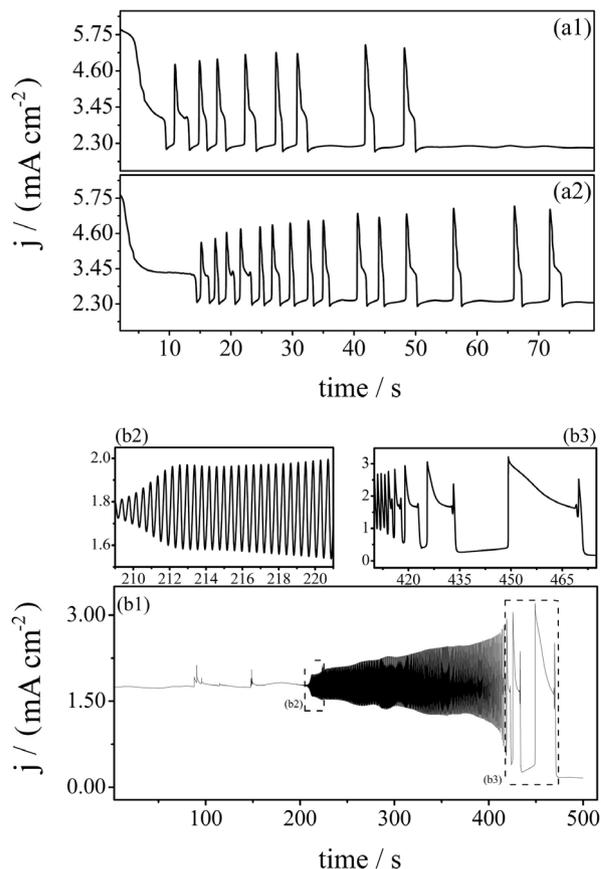


Figure 3. Chronoamperograms obtained for $R = 1$ k Ω and around the (a) first and (b) the second NDR region. Remaining experimental conditions as in Figure 1.

Oscillations in the second NDR region, exemplified here for $E = 1.55$ V and presented in Figure 3(b), set in via a supercritical Hopf bifurcation after a considerably long induction period and evolves spontaneously in time. The spontaneous drift observed in electrochemical systems has been investigated by our Group²³⁻²⁶ and can be generally attributed to a non-controllable surface transformation that slowly drives the system as a bifurcation parameter. In acidic media, the drift has been identified as caused by the slow surface oxidation. As a consequence, the electrode potential slowly increases which favors further oxidation, the whole process occurs in a rather slower time-scale, when compared to the oscillations themselves. This is true for the electrooxidation of small organic molecules in acidic media. For the case of borohydride in alkaline media, it is presently unclear the nature of the surface transformations that causes the drift, moreover, even the transport to/from the electrode surface might play a role in this case. The low amplitude oscillations are rather regular and faster than that found in the first NDR region, reaching frequencies of about 2.5 Hz. The oscillation amplitude slowly grows in time and after about 410 s an abrupt transition to large

amplitude, irregular oscillations takes place. The complex, irregular and slow pattern persists for few cycles (Figure 3(b3)) and the oxidation current goes to zero. At this point, the surface oxidation reaches a point at which it becomes inactive to oxidize borohydride molecules. Other noteworthy differences between the dynamics in the two NDR regions are the higher number of oscillations and the lower current value around which oscillations develop in the second NDR, *cf.* Figure 3(b). Altogether, these differences are related to the mechanism underlying the instabilities and will thus be further discussed later.

Aiming at mapping the region at which current oscillations are found around each NDR, similar experiments for different values of R_{ext} were carried out. Results are given in Figure 4 in terms of a bifurcation diagram in the R vs. E plane, where oscillations around each NDR regions are confined between two values of the applied potential and represented by the blue domains. The oscillatory regions were delimited by a quasi-stationary potential sweep, in a wide potential range. The range of potentials in which oscillations were observed varied, being 7 mV for the smallest and 55 mV for the greatest. What is invariable, nevertheless, is the fact that spontaneous current oscillations emerged in a restricted resistance range.

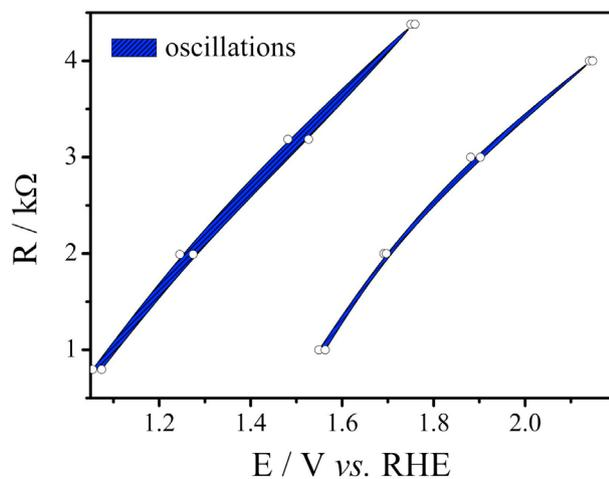


Figure 4. Bifurcation diagram in the R vs. E plane illustrating the existence region of current oscillations. Remaining experimental conditions as in Figure 1.

The existence of a minimum value of the total resistance required for the emergence of oscillations reflects the freedom needed for the electrode potential, an essential variable, oscillates when the applied voltage is kept constant. The fact that current oscillations exist only for finite values of R is characteristic of electrochemical oscillators of the N-NDR type, in contrast to that for HN-NDR oscillators, in which the N-shaped NDR curve is partially hidden

by a secondary process.²⁰⁻²² Therefore, and as already apparent in Figure 4, no oscillations are expected to emerge under galvanostatic regime, which would correspond to a situation in which both R and E go simultaneously to infinite. Figure 5 reinforces this point and shows that no oscillations are found along a slow galvanodynamic sweep. Instead, a nearly 2 V hysteresis between unpoisoned and poisoned states during the positive- and negative-going sweep, respectively, is found. In addition to the experiments presented, electrochemical impedance spectroscopy (EIS) is commonly used to classify electrochemical oscillators, but its application in the present case was not possible due to the difficulty in reaching the steady state. Nevertheless, it should be mentioned the successful application of EIS by Parrou *et al.*²⁷ to the electrooxidation of borohydride on gold.

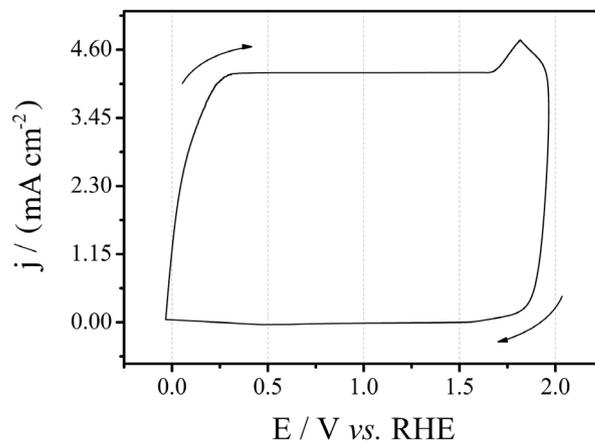


Figure 5. Galvanodynamic sweep at $dI/dt = 0.5 \mu\text{A s}^{-1}$ of the electrooxidation of borohydride under identical conditions than given under potentiostatic regime, *cf.* Figure 1.

From the mechanistic point of view, oscillations around the two NDR regions are very probably caused by different surface chemistries. Abruña and co-workers⁵ have recently identified the two NDR regions and named the first one at lower potentials (ca. 0.8 V) self-cleaning region and second one at ca. 1.2 V the region of slow poison removal, clearly pointing to the distinct time-scales of surface poisoning in each region. Following their interpretation, it is likely that BH_3OH^- acts as the poisoning species in the first NDR region. In addition, given the high potentials around which it occurs, we suggest that the poison that causes the second NDR is probably platinum oxides, similarly to that found for the electrooxidation of hydrogen on platinum.^{28,29} Importantly to the present discussion, the authors⁵ reported the successful implementation of a cleaning procedure that prevents the long-term performance decrease due to the surface poisoning process. The procedure consists of periodically applying short (0.5 s) potential pulses to values

within the second NDR region. The pulses were proven to successfully remove the poisoning species and keep high current densities for the electrooxidation of borohydride. The nature of current oscillations, as seen in Figure 3, closely resembles a periodically poisoning/cleaning process. Of course, the use of autonomous oscillations as a self-cleaning strategy might bring some advantages. In fact, one could envisage the use of spontaneous oscillations to improve the overall performance in practical devices, as already reported for low temperature polymer electrolyte fuel cell operated with H₂/CO mixtures.³⁰⁻³³

The discovery of parameter regions at which the system manifests its intrinsic nonlinear kinetics as well as the description of the self-organized phenomena associated to the kinetics contribute to the current knowledge of the complex electrooxidation of borohydride. A recent example in this direction was reported by Varela and co-workers^{34,35} for the electrooxidation of methanol. Using a comprehensive approach that comprises experiments, modeling and numerical simulations, the authors were able to decouple parallel oxidation pathways that remain otherwise inseparable under regular, non-oscillatory conditions. A just published work by Rustici and co-workers³⁶ reports the presence of oscillations in the production of hydrogen during the homogeneous hydrolysis of borohydride over a wide range of experimental conditions. As emphasized, the results open interesting perspectives, but the chemistry associated to the nonlinear behavior is not understood yet, as in the electrocatalytic oxidation reported here.

Conclusions

We presented in this work novel aspects on the electrooxidation of borohydride on platinum, namely the occurrence of self-organized current oscillations. The spontaneous current oscillations were found in two distinct potential windows and characterized as arising from two negative differential regions (NDR) in N-shaped current-potential curves. The mechanistic origin underlying these instabilities is probably related to the two poisoning steps according to previously published data.⁵ The existence regions of current oscillations were mapped in the potential vs. resistance plane. We are not aware previous reports of current oscillations in this system. From kinetic and mechanistic perspectives, our results add further information on the already intricate set of data obtained under non-oscillatory regime. In terms of practical application, one can think of using self-organized oscillations as a mean to spontaneously and periodically clean the catalyst surface and thus prevent or postpone performance losses. Development through these venues requires however further

experimental and numerical results on this complex system. We are currently working in this direction.

Acknowledgements

E. G. M. and H. V. acknowledge Fundação de Amparo à Pesquisa do Estado de São Paulo (FAPESP) for financial support (grant numbers 2012/07313-1, 2009/07629-6 and 2012/24152-1). H. V. (grant number 306151/2010-3) acknowledges Conselho Nacional de Desenvolvimento Científico e Tecnológico (CNPq) for financial support. The authors express their gratitude to Prof Fabio H. B. Lima for fruitful discussion and encouragement for the work in this topic.

References

1. Demirci, U. B.; *J. Power Sources* **2007**, *169*, 239.
2. Ma, J.; Choudhury, N. A.; Sahai, Y.; *Renewable Sustainable Energy Rev.* **2010**, *14*, 183.
3. Santos, D. M. F.; Sequeira, C. A. C.; *Renewable Sustainable Energy Rev.* **2011**, *15*, 3980.
4. Concha, B. M.; Chatenet, M.; Ticianelli, E. A.; Lima, F. H. B.; *J. Phys. Chem. C* **2011**, *115*, 12439.
5. Finkelstein, D. A.; Letcher, C. D.; Jones, D. J.; Sandberg, L. M.; Watts, D. J.; Abruña, H. D.; *J. Phys. Chem. C* **2013**, *117*, 1571.
6. Gyenge, E.; *Electrochim. Acta* **2004**, *49*, 965.
7. Lima, F. H. B.; Pasqualetti, A. M.; Concha, M. B. M.; Chatenet, M.; Ticianelli, E. A.; *Electrochim. Acta* **2012**, *84*, 202.
8. Concha, B. M.; Chatenet, M.; Maillard, F.; Ticianelli, E. A.; Lima, F. H. B.; de Lima, R. B.; *Phys. Chem. Chem. Phys.* **2010**, *12*, 11507.
9. Finkelstein, D. A.; Da Mota, N.; Cohen, J. L.; Abruna, H. D.; *J. Phys. Chem. C* **2009**, *113*, 19700.
10. Liu, B. H.; Li, Z. P.; Suda, S.; *Electrochim. Acta* **2004**, *49*, 3097.
11. Machado, E. G.; Sitta, E.; de Lima, F. H. B.; Lee, J.; Varela, H.; *Electrochem. Commun.* **2012**, *16*, 107.
12. Batista, B. C.; Sitta, E.; Eiswirth, M.; Varela, H.; *Phys. Chem. Chem. Phys.* **2008**, *10*, 6686.
13. Batista, B. C.; Varela, H.; *J. Phys. Chem. C* **2010**, *114*, 18494.
14. Podlovchenko, B. I.; Manzhos, R. A.; Maksimov, Y. M.; *Russ. J. Electrochem.* **2006**, *42*, 1061.
15. Sitta, E.; Varela, H.; *J. Solid State Electrochem.* **2008**, *12*, 559.
16. Concha, B. M.; Chatenet, M.; Ticianelli, E. A.; Lima, F. H. B.; *J. Phys. Chem. C* **2011**, *115*, 12439.
17. Concha, B. M.; Chatenet, M.; *Electrochim. Acta* **2009**, *54*, 6119.
18. Martins, J. I.; Nunes, M. C.; Koch, R.; Martins, L.; Bazzouai, M.; *Electrochim. Acta* **2007**, *52*, 6443.
19. Koper, M. T. M.; *J. Chem. Soc., Faraday Trans.* **1998**, *94*, 1369.

20. Krischer, K. In *Modern Aspects of Electrochemistry*; Conway, B. E.; Bockris, J. O. M.; White, R., eds.; Springer: USA, 2002, p. 1.
21. Strasser, P.; Eiswirth, M.; Koper, M. T. M.; *J. Electroanal. Chem.* **1999**, *478*, 50.
22. Koper, M. T. M. In *Advances in Chemical Physics*; Prigogine, I.; Rice, S. A., eds.; John Wiley & Sons, Inc.: Hoboken, NJ, USA, 1996, p. 161.
23. Boscheto, E.; Batista, B. C.; Lima, R. B.; Varela, H.; *J. Electroanal. Chem.* **2010**, *642*, 17.
24. Nagao, R.; Sitta, E.; Varela, H.; *J. Phys. Chem. C* **2010**, *114*, 22262.
25. Ferreira, G. C. A.; Batista, B. C.; Varela, H.; *PLoS ONE* **2012**, *7*, 50145
26. Cabral, M. F.; Nagao, R.; Sitta, E.; Eiswirth, M.; Varela, H.; *Phys. Chem. Chem. Phys.* **2013**, *15*, 1437.
27. Parrou, G.; Chatenet, M.; Diard, J. P.; *Electrochim. Acta* **2010**, *55*, 9113.
28. Varela, H.; Krischer, K.; *Catal. Today* **2001**, *70*, 411.
29. Varela, H.; Krischer, K.; *J. Phys. Chem. B* **2002**, *106*, 12258.
30. Lopes, P. P.; Ticianelli, E. A.; Varela, H.; *J. Power Sources* **2011**, *196*, 84.
31. Lu, H.; Rihko-Struckmann, L.; Hanke-Rauschenbach, R.; Sundmacher, K.; *Top. Catal.* **2008**, *51*, 89.
32. Mota, A.; Lopes, P. P.; Ticianelli, E. A.; Gonzalez, E. R.; Varela, H.; *J. Electrochem. Soc.* **2010**, *157*, 1301.
33. Zhang, J.; Datta, R.; *Electrochem. Solid-State Lett.* **2004**, *7*, A37.
34. Nagao, R.; Cantane, D. A.; Lima, F. H. B.; Varela, H.; *Phys. Chem. Chem. Phys.* **2012**, *14*, 8294.
35. Nagao, R.; Cantane, D. A.; Lima, F. H. B.; Varela, H.; *J. Phys. Chem. C* **2013**, *117*, 15098.
36. Budroni, M. A.; Biosa, E.; Garroni, S.; Mulas, G.; Marchettini, N.; Culeddu, N.; Rustici, M.; *Phys. Chem. Chem. Phys.* **2013**, *in press*, DOI: 10.1039/c3cp53302f.

Submitted: August 6, 2013

Published online: October 2, 2013

FAPESP has sponsored the publication of this article.